AIP | Applied Physics Letters

Atomic structure of (110) anti-phase boundaries in GaP on Si(001)

A. Beyer, B. Haas, K. I. Gries, K. Werner, M. Luysberg, W. Stolz, and K. Volz

Citation: Applied Physics Letters **103**, 032107 (2013); doi: 10.1063/1.4815985
View online: http://dx.doi.org/10.1063/1.4815985
View Table of Contents: http://scitation.aip.org/content/aip/journal/apl/103/3?ver=pdfcov
Published by the AIP Publishing

Atomic structure of (110) anti-phase boundaries in GaP on Si(001)

A. Beyer,[1] B. Haas,[1] K. I. Gries,[1] K. Werner,[1] M. Luysberg,[2] W. Stolz,[1] and K. Volz[1]
[1]*Materials Science Center and Faculty of Physics, Philipps-University Marburg, Hans-Meerwein-Strasse, DE-35032 Marburg, Germany*
[2]*Peter Grünberg Institut (PGI-5), Forschungszentrum Jülich, DE-52425 Jülich, Germany*

(Received 22 April 2013; accepted 29 June 2013; published online 17 July 2013)

High quality III/V-layers grown on Si enable a variety of optoelectronic devices. The performance of such devices is limited by anti-phase domains forming at monoatomic steps on the Si-surface. To date the atomic structure of anti-phase boundaries, which affects the charge distribution at polar interfaces, is unknown. Here, we use C_S-corrected scanning transmission electron microscopy to reveal the atomic structure of the anti-phase boundaries in III/V-semiconductors, choosing GaP as a model system. We observe boundaries on (110) lattice planes which are atomically abrupt and also facetted ones, which introduces locally charged regions influencing device performance. © *2013 AIP Publishing LLC*. [http://dx.doi.org/10.1063/1.4815985]

High-quality growth of III/V-material on Si-substrates offers great opportunities for future devices like monolithically integrated lasers[1,2] or high electron mobility transistors.[3] GaP is of special interest, because of its lattice constant being similar to that of Si. Therefore, the formation of strain induced defects can be neglected. Nevertheless, the heteroepitaxy of polar material on non-polar substrate is challenging, as the interface is not automatically charge neutral, and anti-phase domains (APDs) can form at monoatomic steps on the substrate.[4] These APDs can influence the performance of a later device adversely because of the homopolar bonds they introduce at their boundaries. Growth conditions to minimize the amount of APDs were already proposed for InP (Ref. 5) and GaP (Refs. 6 and 7) on Si. In previous work we already presented the size and shape of the remaining APDs in GaP grown on nominally exact Si(001) on a nanometer scale by TEM[8] utilizing conventional dark field imaging with optimized tilting conditions.[9] As basis for the current result, the main findings on the APD shape will be summarized briefly. In the following, the growth direction will be defined as [001], the intentional 0.1° offcut was chosen into the [110]-direction, and therefore the step edges run along the perpendicular [-110]-direction. We will maintain this nomenclature for the crystallographic direction of the Si for the grown GaP layer as well, irrespective of its polarity. The residual APDs follow the step edges of the substrate, which exhibit a D_A-like surface step configuration prior to the GaP growth.[10,11] Moreover, the APDs show an anisotropic shape: viewed along the steps they run on {110}-planes, while they annihilate on {112}-planes viewed along the orthogonal [110]-direction. Hence, macroscopically charge neutral boundaries remain. The exact atomic structure of the anti-phase boundaries (APBs) framing the APDs is yet unknown, because of the limited resolution of the dark field method applied previously.[8] However, this exact atomic structure is important, as it influences the charge distribution in the interface region. For other materials like ceramics and perovskites C_S-corrected scanning transmission electron microscopy (STEM) has proven to be a valuable tool to investigate the structure of APBs.[12,13] In this paper we use C_S-corrected high angle annular dark field (HAADF) measurements to investigate the (110) APBs in GaP grown on Si on an atomic scale.

GaP layers were grown via metal organic vapor phase epitaxy (MOVPE) in an Aixtron 200 GFR reactor on Si(001) substrates with an intentional miscut of 0.1° into the [110]-direction which still falls in the specification of the complementary metal oxide semiconductor (CMOS) process. Special growth conditions were applied which result in high quality GaP layers and self-annihilation of the present APDs after several ten nanometers.[6] Electron transparent samples were prepared in cross-sectional and plan-view (PV) geometry by conventional mechanical thinning followed by argon ion milling at an incident angle of 5°. The STEM measurements were carried out in a JEOL ARM 200F, a JEOL 2200 FS, and a FEI Titan 80–300, all equipped with probe aberration-correctors. The microscopes operate at acceleration voltages of 200 kV and 300 kV, respectively. For comparison with the experimental findings, theoretical HAADF-intensities were calculated using the commercially available HREM package which utilizes a FFT-multislice algorithm[14] and an absorptive potential approximation.[15] The microscope parameters, like the semi-convergence angle and the angular detection range, were measured during the experiments and taken into account for the simulation. Supercells containing APDs with different boundary configurations were constructed in a virtual crystal approximation (VCA), in which all atoms are situated at their perfect lattice sites.

Figure 1(a) depicts a HAADF-image of a GaP TEM-foil prepared in PV geometry, where the viewing direction equals the growth direction [001]. In the visible region the foil-thickness can be regarded as constant, as the HAADF-intensity does not change significantly across the image. Due to the small probe size achieved by the usage of the C_S-corrector, the Ga- and P-sublattices can clearly be distinguished, although the atom spacing is only 0.19 nm. Due to the Z^2-dependence[16] of the intensity, atomic columns of Ga appear brighter than those of P. The image is divided horizontally by an APB, which runs along the [-110]-direction following a step edge of the formerly underlying Si-substrate. The width of the APB increases from left to right, which is

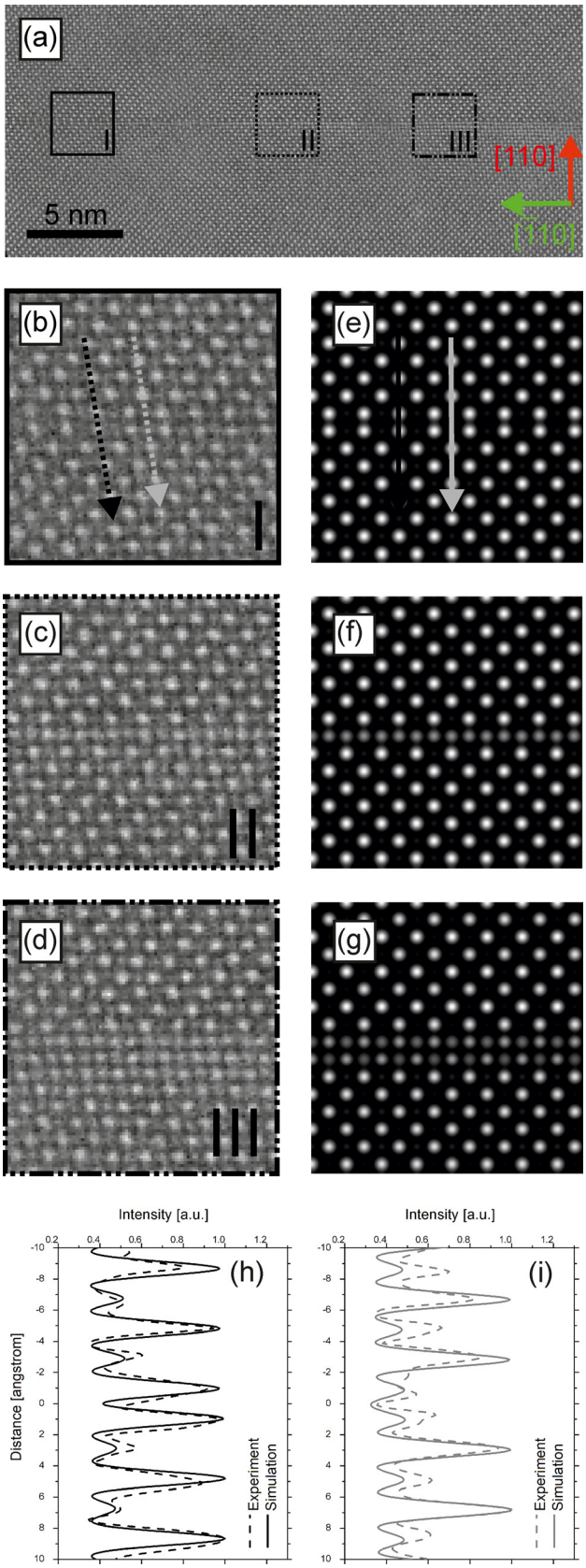

FIG. 1. High angle annular dark field image of a GaP layer on Si in PV geometry: High resolution image of an anti-phase boundary along the [110]-direction of the Si substrate (a). (b) An enlarged view of a region where the APB exhibits minimum thickness. Regions with a thickness of one and two atomic layers are depicted in (c) and (d), respectively. The corresponding simulations can be found in (e)–(g). Intensity profiles perpendicular to the abrupt experimental (dashed line) and simulated (solid line) boundary reveal the wrong Ga-Ga bonds (h) and P-P bonds (i).

seen in more detail in the enlarged images of regions I-III in Figures 1(b)–1(d). The corresponding simulations can be found in Figures 1(e)–1(g). The simulated intensities were derived from crystal models of APBs running on a {110}-plane with different boundary configurations that will be described in more detail later. The thickness for the simulation was chosen to 20 unit cells, which is approximately 11 nm, to fit the experimental images. Ball and stick models which represent the used structures can be found in Figure 2. In the region shown in Figure 1(b) the boundary exhibits its minimum thickness and is atomically abrupt. The visible image distortion may be caused by mechanical drift of the specimen stage during the scanning process. The alternating wrong bonds between two Ga- and two P-atoms can, however, be seen directly in the image and in the intensity profiles perpendicular to the boundary (dashed lines in Figs. 1(h) and 1(i)). The simulated image (Fig. 1(e)) derived from the model of a perfect {110}-boundary (Fig. 2(a)) resembles the experimental data very well, which can be seen in more detail in the intensity profiles (solid lines in Figs. 1(h) and 1(i)). In Figure 1(c) the APB has a thickness of one atomic layer and

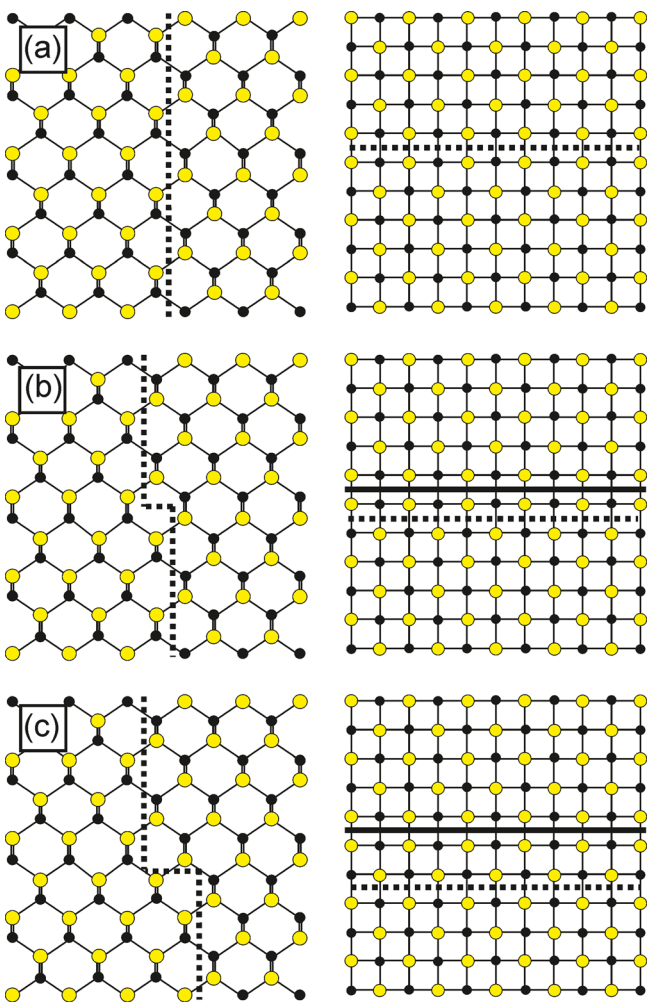

FIG. 2. Ball and stick model of the supercells used for simulation of HAADF-intensities depicting an abrupt boundary (a), a jump by one atomic plane (b), and a jump by two atomic planes (c). The left column shows the [-110]-projections while the right column shows the corresponding [001]-projections. The solid line visualizes the position of the boundary at the entrance surface while the dashed line represents the boundary at the lower surface. The bright dots represent Ga- and the dark ones P-atoms.

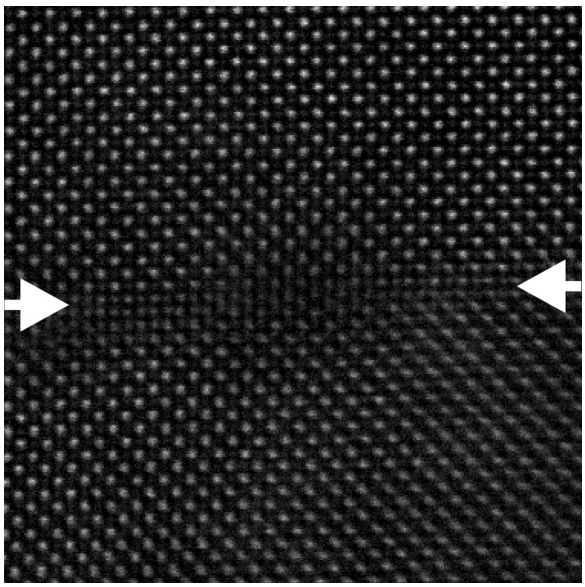

FIG. 3. HAADF-image of an anti-phase boundary in PV geometry which jumps by one {110} plane (a). The positions of the boundary on the left and the right side of the picture are marked by arrows.

appears as a line of medium intensity. This may be explained by the fact that the APB is not fixed on a {110}-plane but jumps from one to another {110}-plane in viewing direction. The simulation taking such a jump by one atomic plane in the center of the model (Fig. 2(b)) into account can be found in Figure 1(f). The plane of medium intensity is clearly observable and exhibits the mean intensity of pure Ga and P as the columns in viewing direction are occupied by half Ga and half P. Further thickness dependent simulations show that this linear behavior holds for sample thicknesses below approximately 30 nm. Due to the idealized model in which the jump occurs directly in the center of the crystal (see Fig. 2(b)), the atoms along the boundary have the same intensity. As the boundary can occur at another height in the real case, the crystal consists of different fractions of phase and anti-phase. Therefore, the neighboring atoms show alternating intensity. The boundary region enlarged in Figure 1(d) has a width of two atomic layers. This can be reproduced well by the simulation (Fig. 1(g)) derived from the crystal model containing a jump by two atomic planes (Fig. 2(c)). This shows that increasing the width of a jump just straight forwardly results in the appearance of more layers of intermediate intensity. In the region of the APB imaged in Figure 3 a jump by one {110}-plane is directly observable. The horizontal position of the boundary on each side of the image is marked by an arrow.

To confirm the presence of the jumps the investigation of cross-section samples in a ⟨110⟩-projection is necessary. Due to the smaller atom-spacing of 0.14 nm it is more challenging to resolve the two sublattices. Figure 4(a) shows a HAADF-image in [-110]-projection, viewing along the steps of the Si-substrate. The different atoms of the dumbbells are clearly resolved, so that the polarity is visible directly. This becomes more evident in the enlarged regions and the corresponding ball and stick models that are depicted right from the image. On the left side of the HAADF-image (region I) the crystal is Ga-polar while it is P-polar on the right side

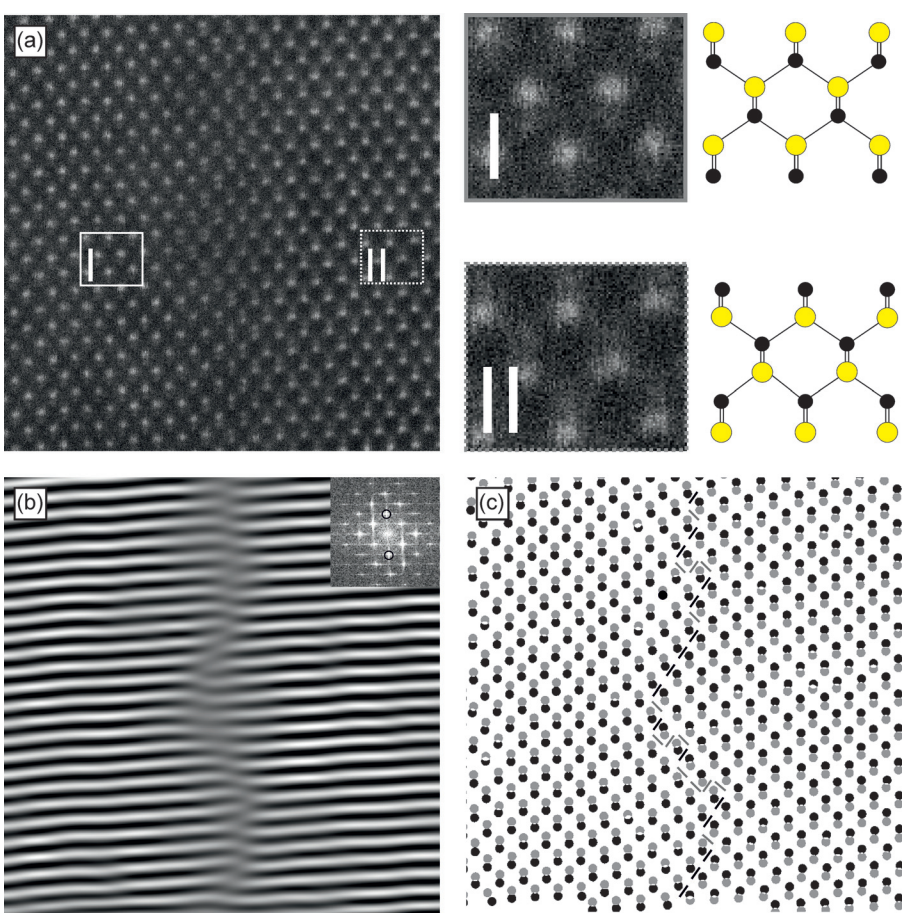

FIG. 4. HAADF-image of a comparable boundary in cross-sectional geometry (a). The path of the boundary becomes more obvious in Fourier-filtered image (b), which is obtained by applying a mask around the (002) spots. In the digital map (c) Ga-columns are represented by grey dots, while P-atoms are represented by black ones. The 14 Ga-Ga and 16 P-P wrong bonds are marked by lines in the corresponding colors.

(region II), which is the main phase of the crystal. This is in agreement with previous convergent beam electron diffraction (CBED)-measurements of GaP/Si-samples.[8,10] The two domains are separated by a boundary whose course becomes more evident in the Fourier-filtered image (Fig. 4(b)). This image was obtained by putting a mask around the (002)-spots in the Fourier-transformed image, as the {002}-planes are most sensitive to the polarity of the III/V-material. The Fourier-transformation and the size of the used mask are shown in the inset. The Fourier-filtered image reveals an APB, which does not run straight on a charge neutral {110}-plane but is facetted on higher indexed planes, confirming also the conclusions drawn from Figure 1. The boundary regions with different inclinations with respect to the growth direction macroscopically result in a boundary parallel to {110} which is observable in conventional darkfield TEM.[8] This faceting is surprising as preliminary *ab initio* calculations show the {110}-boundary to be energetically most favorable.[17] In addition, the charge distribution of the GaP/Si-layer is affected by this faceting: APBs on {110}-planes are macroscopically charge neutral, while APBs on higher index planes exhibit some charge. To quantify the actual charge of the investigated boundary, the amount of wrong bonds of different type has to be determined. To facilitate this, the experimental image is treated in a digital way, in which the column of the dumbbell, which has the higher intensity, is regarded as fully occupied with Ga and the other one with P. Due to this simplification the information in viewing direction is lost. The result of this treatment is shown in Figure 3(c), where the grey dots represent Ga and the black dots P. The resulting wrong bonds are marked by lines with the corresponding color. It is notable that especially the wrong P-P bonds lie on {111}-planes. The investigated region exhibits 16 P-P bonds and 14 Ga-Ga bonds and is therefore macroscopically almost charge neutral, which confirms the macroscopic findings.[8] Unequivocally, the faceting results in an accumulation of local charges which can influence the performance of a device adversely. This study shows that the observed APB configuration in [110]-projection is not fixed, as regions with a uniform thickness in plane view orientation exhibit abrupt boundaries as well as ones with finite thickness. Therefore, jumps from one plane to another as well as the observed faceting may occur statistically, driven by the temperature during the growth. Future work will be dedicated to the understanding of the influence of the growth temperature on the atomic structure of the APBs. The atomic structure of the APBs as found here could, however, be exploited via the application of higher temperatures to increase the probability of jumps and therefore the chance that two boundaries meet each other and annihilate, which would reduce the amount of wrong bonds.

In conclusion, we were able to characterize the structure of APBs in the GaP/Si-system on an atomic scale via C_S-corrected HAADF-imaging in concordance with adequate simulation. The APBs are not atomically abrupt but can have finite thicknesses due to random jumps between {110}-planes occurring during the growth process.

We gratefully acknowledge financial support from the German Science Foundation (DFG). Also, we appreciate support from JEOL using the ARM.

[1]B. Kunert, K. Volz, J. Koch, and W. Stolz, Appl. Phys. Lett. **88**, 182108 (2006).
[2]S. Liebich, M. Zimprich, A. Beyer, C. Lange, D. J. Franzbach, S. Chatterjee, N. Hossain, S. J. Sweeney, K. Volz, B. Kunert, and W. Stolz, Appl. Phys. Lett. **99**, 071109 (2011).
[3]L. Desplanque, S. El Kazzi, C. Coinon, S. Ziegler, B. Kunert, A. Beyer, K. Volz, W. Stolz, Y. Wang, P. Ruterana, and X. Wallart, Appl. Phys. Lett. **101**, 142111 (2012).
[4]H. Kroemer, J. Cryst. Growth **81**, 193 (1987).
[5]G.-P. Tang, A. Lubnow, H.-H. Wehmann, G. Zwinge, and A. Schlachetzki, Jpn. J. Appl. Phys. **31**, L1126 (1992).
[6]K. Volz, A. Beyer, W. Witte, J. Ohlmann, I. Németh, B. Kunert, and W. Stolz, J. Cryst. Growth **315**, 37 (2011).
[7]I. Németh, B. Kunert, W. Stolz, and K. Volz, J. Cryst. Growth **310**, 1595 (2008).
[8]A. Beyer, I. Németh, S. Liebich, J. Ohlmann, W. Stolz, and K. Volz, J. Appl. Phys. **109**, 083529 (2011).
[9]I. Németh, B. Kunert, W. Stolz, and K. Volz, J. Cryst. Growth **310**, 4763 (2008).
[10]A. Beyer, J. Ohlmann, S. Liebich, H. Heim, G. Witte, W. Stolz, and K. Volz, J. Appl. Phys. **111**, 083534 (2012).
[11]S. Brückner, H. Döscher, P. Kleinschmidt, O. Supplie, A. Dobrich, and T. Hannappel, Phys. Rev. B **86**, 195310 (2012).
[12]L. Q. Wang, B. Schaffer, I. MacLaren, S. Miao, A. J. Craven, and I. M. Reaney, J. Phys.: Conf. Series **371**, 012036 (2012).
[13]S. Li, Q. Gao, J. Li, X. He, Q. Zhang, C. Li, Y. Shen, L. Gu, Y. Yao, Y. Wang, R. Yu, X. Duan, and Y. Ikuhara, Mater. Express **2**, 51 (2012).
[14]K. Ishizuka, Ultramicroscopy **90**, 71 (2002).
[15]C. R. Hall and P. B. Hirsch, Proc. R. Soc. London, Ser. A **286**, 158 (1965).
[16]S. Pennycook and D. Jesson, Ultramicroscopy **37**, 14 (1991).
[17]O. Rubel and S. D. Baranovskii, Int. J. Mol. Sci. **10**, 5104 (2009).